# The Nature of Magnetoelectric Coupling in $Pb(Zr,Ti)O_3$–$Pb(Fe,Ta)O_3$

*Donald M. Evans, Marin Alexe, Alina Schilling, Ashok Kumar, Dilsom Sanchez, Nora Ortega, Ram S. Katiyar, James F. Scott, and J. Marty Gregg**

The last decade has seen an explosion of research activity in multiferroic materials. This has partly been driven by fundamental interest, but partly also by the exciting prospect of new forms of functional devices. In most cases, envisioned device performance requires distinct room temperature coupling between the magnetic moment and the electrical polarization: under ambient conditions, an applied electric or magnetic field must simultaneously alter both the material's electrical dipole configuration and its magnetic state. A key stumbling block for progress has been that, despite concerted effort, very few single-phase materials have been discovered in which strongly coupled behavior has been categorically and unequivocally established at room temperature. One candidate system is the $Pb(Zr,Ti)O_3$–$Pb(Fe,Ta)O_3$ (PZTFT) solid solution, where promising initial observations have been made, which demand more careful and systematic examination. In this paper, the ferroelectric behavior and dielectric response of single crystal PZTFT lamellae have been mapped as a function of applied magnetic field. Significant switching of ferroelectric domains using magnetic fields was observed; in addition, strong hysteretic magnetocapacitance effects were noted. A Landau free energy approach was used to demonstrate that $P^2M^2$ coupling behavior was generally evident, but that for magnetic fields applied perpendicular to the lamella surface (those responsible for ferroelectric switching), asymmetric coupling terms (such as $PM$) were more important.

Dr. D. M. Evans, Dr. A. Schilling, Prof. J. M. Gregg
Centre for Nanostructured Media, School of Maths and Physics
Queen's University Belfast
Belfast BT7 1NN, Northern Ireland, UK
E-mail: m.gregg@qub.ac.uk

Prof. M. Alexe
Department of Physics
University of Warwick
Coventry CV4 7AL, UK

Dr. A. Kumar
National Physical Laboratory
New Delhi, Delhi 110012, India

Dr. D. Sanchez, Dr. N. Ortega, Prof. R. S. Katiyar
Institute for Functional Nanomaterials
University of Puerto Rico, PO Box 23334
San Juan, PR 00931-3334, USA

Prof. J. F. Scott
School of Chemistry
University of St Andrews
St Andrews KY16 9ST, Scotland, UK

Prof. J. F. Scott
School of Physics and Astronomy
University of St Andrews
North Haugh, St Andrews KY16 9SS, Scotland, UK

In 1964, Hans Schmid was the first to observe the simultaneous existence of ferroelectricity and ferromagnetism in a single material: the synthetic boracite $Ni_3B_7O_{13}I$.[1] Two years later, Ascher et al.[2] revealed that the magnetic moment and polarization in this boracite were coupled, such that an applied magnetic field could cause complete reversal of the ferroelectric polarization. This breakthrough discovery was somewhat academic, until the recent renaissance of interest in multiferroics prompted more serious consideration of the device potential of the magnetoelectric coupling phenomenon.[3,4]

Given the immense effort devoted by Schmid and co-workers toward finding the first single-phase multiferroic, it is a little ironic that most recent progress toward magnetoelectric applications has primarily involved mixed-phase systems in composite structures.[5–13] Single-phase materials unfortunately usually suffer from two main drawbacks: first, the vast majority of them are only multiferroic at cryogenic temperatures;[14–20] second, their magnetoelectric coupling coefficients tend to be somewhat lower than in dual-phase multilayers. In fact, Ramesh and co-workers have recently even suggested that the archetypical room temperature single-phase multiferroic, $BiFeO_3$, might most usefully be used in a composite device.[21]

Nevertheless, there are specific applications and device geometries in which a single layer of a phase-pure magnetoelectric multiferroic would still be desirable. This is particularly true when seeking to use multiferroics as insulating layers in tunnel junction-based devices (such as the spin-filter suggested by Bibes,[3] as the thicknesses needed for tunneling are not commensurate with those needed for dynamic interlayer elastic coupling. Equally, in memory applications, low power electrical switching of magnetization could be significantly faster in single-phase multiferroics than in composites (supersonic switching is possible, if electronic coupling mechanisms are active). Thus, the drive to discover new phase-pure room temperature multiferroics, beyond $BiFeO_3$, continues. Several candidate materials have recently been identified, such as the Bi-based aurivillius oxides,[22] $GaFeO_3$ thin films,[23] and perovskite oxides within the PZTFT solid solution.[24–28] The properties of this latter group will be the focus of this article. Some relevant observations have already been made: after initial reports in which room temperature multiferroicity and magnetoelectric coupling had been suggested[24,27] the wider phase transition behavior in the PZTFT solid solution was investigated by Schiemer et al.[26] By monitoring elastic resonance frequency, magnetization, and dielectric loss they

established that ferroelastic, magnetic, and ferroelectric anomalies occurred at the same temperatures; such coincident phase transitions strongly suggest coupling among all three ferroic order parameters. A number of theoretical investigations[29–31] have attempted to explain the anomalously high ferromagnetic Curie temperature in this material. In addition, Glinchuk et al.[31] have predicted the size of the coupling and in what compositions its existence is expected. However, categorical experimental information on the exact form of the coupling is still lacking.

Here, we report the manner in which applied magnetic fields change both the ferroelectric behavior (domain states) and dielectric response of single crystal PZTFT lamellae. We observe that ferroelectric switching, in the plane of the lamella, can be induced by perpendicular magnetic fields applied parallel to a pseudocubic $[\bar{1}10]_{pc}$ direction; moreover, we observe distinct magnetocapacitance phenomena, which vary as a function of the orientation of the applied magnetic field. Free energy analysis of the magnetocapacitance suggests that biquadratic $P^2M^2$ coupling is most significant when fields are applied in the plane of the lamella, but least significant when applied in the perpendicular orientation, where asymmetric terms (such as bilinear *PM* coupling) become more important. This is consistent with the magnetic field-induced ferroelectric switching observed.

To enable our investigation, thin single crystal platelets, or lamellae, were cut from the interior of individual grains of PZTFT ceramic using focused ion beam (FIB) milling. As has been done in previous research,[32–34] these lamellae were integrated into simple capacitor devices by placing them across an interelectrode gap (of the order of a few microns in thickness) between coplanar thin film platinum electrodes. The crystallographic orientation was determined by FIB-cutting a second lamella, parallel to the first, from the same PZTFT grain, transferring onto a carbon-coated 3 mm diameter grid and investigating using electron diffraction, in a 200 kV field emission transmission electron microscope. All data presented herein relate to lamellae cut parallel to $\{\bar{1}10\}_{pc}$ planes and oriented in the capacitor structure with a $[001]_{pc}$ direction parallel to the electrode–ferroelectric interface and a $[110]_{pc}$ direction perpendicular to the electrode–ferroelectric interface and parallel to the electric field, when a potential difference was applied across the platinum electrodes. Successful device fabrication and basic magnetoelectric coupling were checked: remanent domain configurations, mapped by piezoresponse force microscopy (PFM), after switching from a fully poled initial state with both electric and magnetic fields, were found to be comparable (**Figure 1**). It was noted, however, that after the initial switching had been induced magnetically, subsequent reversal of the magnetic field produced progressively more modest changes in the ferroelectric domain configuration; the fully poled initial state could not be recovered unless an electric field was used. Currently, this observation is not understood, but such "fatigue" in the magnetically induced ferroelectric switching may be a feature of local elastic field interactions between ferroelastic domain variants and an associated progressive accumulation of pinned domain walls.

Magnetocapacitance was monitored using an Agilent bridge E4980A Precision inductance, capacitance, and resistance (LCR) meter; capacitors were mounted in a cryostat with in situ magnetic field capability. Initial measurements were taken without any magnetic field, to confirm the double-peaked capacitance–voltage ($C(V)$) response characteristic of a switching ferroelectric. As can be seen in **Figure 2**a, the magnitude of the peaks in the $C(V)$ response were approximately the same at positive and negative voltage. When these measurements were repeated under an applied magnetic field of 1 T (oriented along $[\bar{1}10]_{pc}$, perpendicular to the plane of the PZTFT lamella—the same direction as had been responsible for the magnetic-field-induced ferroelectric switching in Figure 1), changes in the $C(V)$ characteristic resulted: the heights of the peaks in capacitance at positive and negative voltage became distinctly different. In the example shown in Figure 2a, the capacitance peak in the positive sense of applied voltage was suppressed relative to that measured in the negative sense. This relative difference was reversed when the sense of the magnetic field was reversed; however, somewhat consistent with observations of magnetic-field-induced switching of ferroelectric domains, the extent to which the magnetic field altered the relative heights of the peaks in capacitance progressively diminished as the sense of the magnetic field was repeatedly reversed.

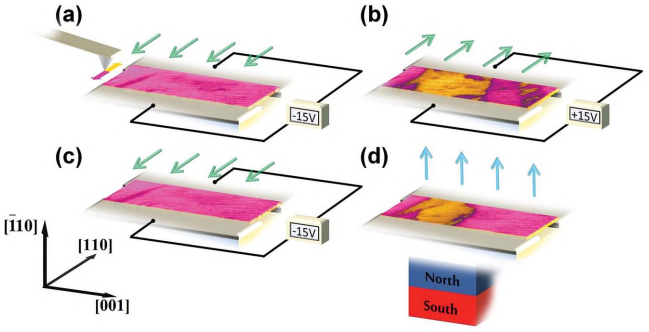


**Figure 1.** Magnetic and electric fields both cause ferroelectric switching. a–d) Piezoresponse force microscopy images (phase superimposed on amplitude) of a lead zirconate titanate-lead iron tantalate (PZTFT) single crystal lamella integrated into a simple coplanar device after the following bias levels and magnetic fields had been applied at room temperature: (a) −15 V, (b) +15 V, (c) −15 V, (d) "+" 3 kOe perpendicular to the lamella (parallel to a $[\bar{1}10]_{pc}$ crystallographic direction in the PZTFT). The magnetic field in this orientation has caused switching of ferroelectric domains comparable to that caused by the +15 V bias. The lamella dimensions were typically ≈10 μm × 5 μm × 0.3 μm.

Capacitance was then monitored in the absence of a dc voltage bias, but with varying magnetic field. At a range of temperatures (between 10 and 305 K), the magnetic field was scanned from 0 to +H to −H and back to 0 at a speed of 150 Oe $s^{-1}$, in three orthogonal directions ($[001]_{pc}$, $[110]_{pc}$, and $[\bar{1}10]_{pc}$ as shown in Figure 1). As a representative illustration, datasets taken at 150 K and 100 kHz are shown in Figure 2b–d. 150 K is sufficiently cold to avoid thermal measurement drift and safely away from any of the phase transition temperatures identified in previous work;[26] 100 kHz is a sufficiently high frequency that space–charge artifacts, which can contribute to magnetocapacitance,[35] are avoided. As can be seen in the figure, all magnetocapacitance functions were found to be hysteretic; in addition, for all orientations, the absolute changes in capacitance induced by the applied magnetic fields were large (significant fractions of the changes caused by electric fields

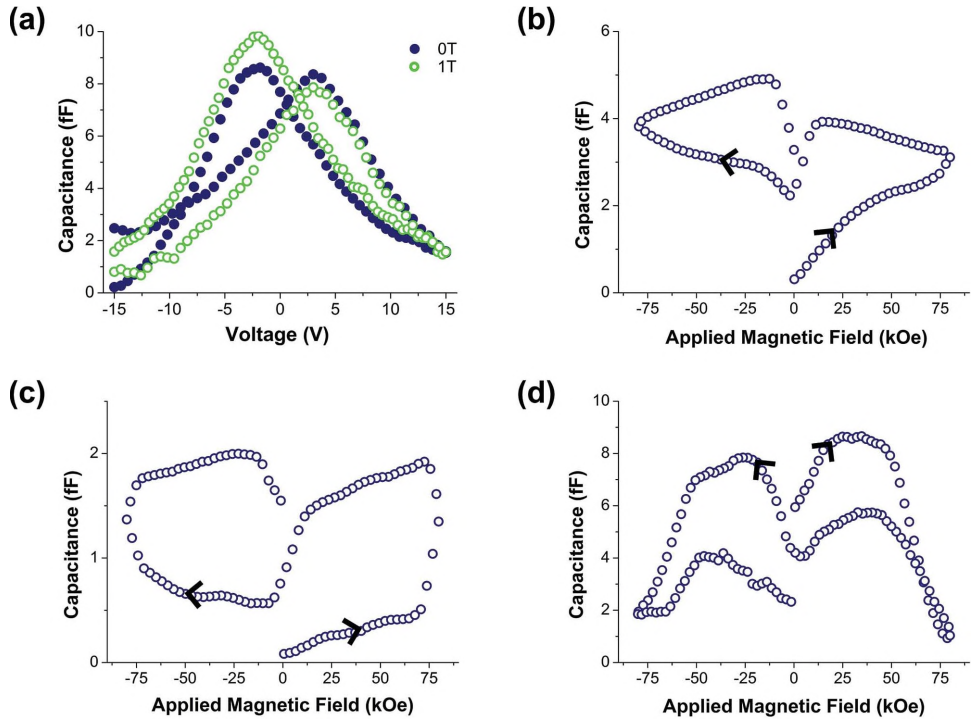


**Figure 2.** Effects of magnetic field on capacitance at 150 K. Magnetic fields were found to alter the way in which capacitance varied as a function of voltage ($C(V)$) in the PZTFT single crystal capacitor a). The low field capacitance was monitored as a function of magnetic field only, applied parallel to the $[001]_{pc}$, $[110]_{pc}$, and $[\bar{1}10]_{pc}$ directions (b), c), and d), respectively) as defined in Figure 1. In all cases, the magnetic field caused significant changes in capacitance and the response was hysteretic. For fields applied along $[\bar{1}10]_{pc}$, capacitance changes were comparable with those associated with ferroelectric switching in the $C(V)$ response.

during switching, seen in the $C(V)$ response, Figure 2a). The detailed form of the magnetocapacitance function clearly also varied with the orientation of the applied field.

Insight can be gained by considering the dielectric susceptibility (which scales with the capacitance) derived from a compact Landau free energy ($G$) expression given as follows:

$$G = \sum_{i=1}^{\infty} A(i)P^{2i} - E \cdot P + \sum_{j=1}^{\infty} B(j)M^{2j} - H \cdot M + \sum_{k=1}^{\infty} C(k)\varepsilon^{2k} - S \cdot \varepsilon + \sum_{i,j,k=0}^{\infty} D(i,j,k)P^{i}M^{j}\varepsilon^{k} \quad (1)$$

The first pair of terms in this expression captures the symmetric energy expansion in polarization ($P$) and the work done by the electric field ($E$); the second pair of terms captures the equivalent in magnetization ($M$) and magnetic field ($H$) and the third pair in strain ($\varepsilon$) and stress ($S$). The last term is a summation of all possible energy contributions from all possible combinations of coupling among polarization, magnetization, and strain. $A(i)$, $B(j)$, $C(k)$, and $D(i,j,k)$ represent constants, the values of which change with different values of $i$, $j$, and $k$. Despite its coarse nature, this equation should capture the essence of multiferroic behavior, even if underlying order parameters are not completely explored and defined: for example, the use of $M$ alone to describe magnetization does not distinguish between order parameters associated with spin clustering of $Fe^{+3}$ ions and possible canted antiferromagnetism in PZTFT. A more complete description should probably include terms such as $(L \times M)P$ and $(L \times M)P^2$, where $L$ is sublattice magnetization and $M$ is weak ferromagnetism from canting, as has been emphasized by Fox, Tilley, Scott, and Guggenheim.[36] However, while such terms are probably important in pure Pb(Fe,Nb)$O_3$ (Peng et al.[37] have shown that both clustering and canting contribute to the net magnetization) they may not be as key in PZTFT: four different ions on the B-site suggest that clustering is apt to dominate. For the moment all such subtleties are subsumed within the order parameter $M$.

Under equilibrium conditions ($dG/dP = 0$), an expression for the electric field can readily be obtained from Equation (1). Hence, an expression for the inverse dielectric susceptibility ($dE/dP = \chi^{-1}$) can be given as

$$\chi^{-1} = \sum_{i=1}^{\infty} A(i)2i(2i-1)P^{2i-2} + \sum_{i,j,k=0}^{\infty} D(i,j,k)i(i-1)P^{i-2}M^{j}\varepsilon^{k} \quad (2)$$

If we now consider how the inverse dielectric susceptibility varies as a function of magnetic field, the following expression is obtained

$$\frac{d\chi^{-1}}{dH} = \sum_{i,j,k=0}^{\infty} D(i,j,k)i(i-1)P^{i-2}j\frac{dM}{dH}M^{j-1}\varepsilon^{k} \quad (3)$$

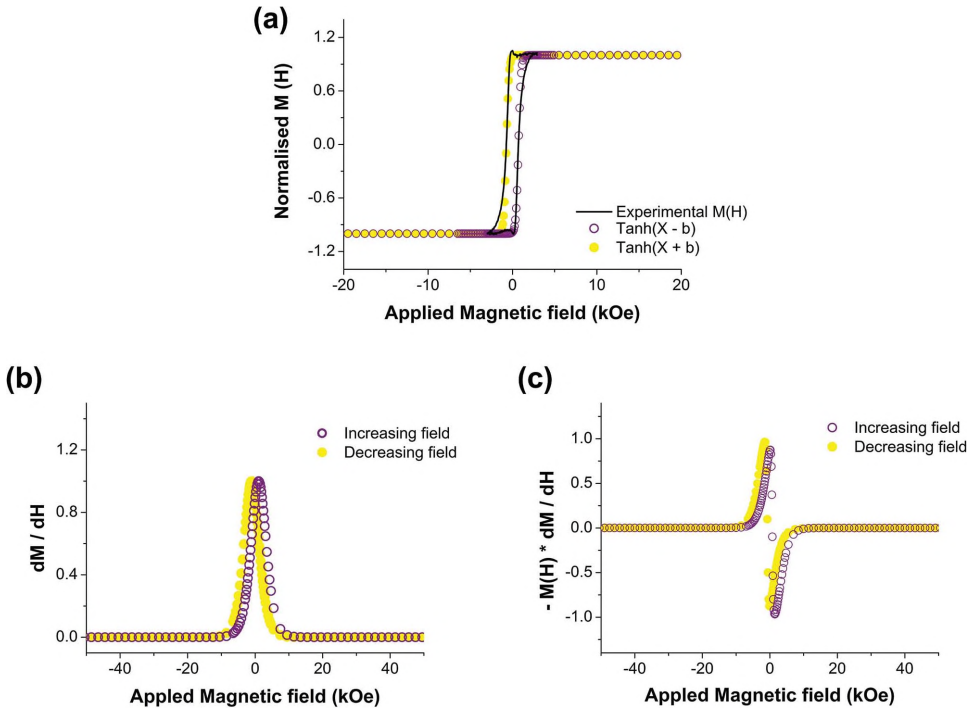


**Figure 3.** Analysis of the room temperature magnetization of the bulk PZTFT ceramic. To gauge the broad manner in which the magnetic field might affect capacitance ($C(H)$), the room temperature magnetization as a function of field in the bulk ceramic PZTFT was first fitted to two tanh functions a). This allowed ready calculation of $dM/dH$ and $-M(dM/dH)$ as a function of magnetic field [b) and c), respectively]. If $P^2M^2$ coupling is present in the material (which is always allowed by symmetry), then expectations from Landau free energy expansions are that $dC^{-1}/dH$ should be proportional to $M(dM/dH)$.

Thus, importantly, by taking the derivative of the inverse susceptibility (which scales as the inverse capacitance) with respect to magnetic field, and examining it as a function of magnetic field, we can directly and specifically probe the coupling terms in the Landau free energy expansion.

Let us consider a simplified form of this equation where $k = 0$ (in other words where strain is not explicitly involved in the multiferroic coupling energy). If linear $PM$ coupling were the only active behavior, $(i - 1)$ would be zero and hence the $d\chi^{-1}/dH$ response should be zero for all applied magnetic fields; if quadratic–linear coupling of the form $P^2M$ were the only active coupling, $d\chi^{-1}/dH$ should be proportional to $dM/dH$; equally, if dominated by biquadratic terms ($P^2M^2$ which are always symmetry allowed) then it should be primarily proportional to $M(dM/dH)$.

To examine the form that $M$ and $dM/dH$ based functions might have in PZTFT, the magnetization with applied field was measured for the bulk ceramic (the measurement of the $M(H)$ behavior in the PZTFT lamella was experimentally beyond our capabilities). This is presented in **Figure 3**a along with tanh fits which allowed analytical determination of $dM/dH$ (Figure 3b) and hence of $-M(dM/dH)$ (Figure 3c). Comparisons of these functions with those experimentally determined from measured magnetocapacitance data (plots of $d(C^{-1})/dH$ against $H$, **Figure 4**a–c) are quite revealing: with magnetic fields applied parallel to $[001]_{pc}$ (in the plane of the lamella, parallel to the dielectric–electrode interface), the maxima and minima in $d(C^{-1})/dH$ either side of $H = 0$, for both increasing and decreasing magnetic fields, show strong similarities to the primary features in the $-M(dM/dH)$ function plotted in Figure 3c. As discussed above, this is consistent with significant biquadratic $P^2M^2$ coupling from consideration of Equation (3). For magnetic fields applied parallel to the $[110]_{pc}$ crystallographic direction (in the plane of the lamella, perpendicular to the dielectric–electrode interface) similar features can be seen, but they are less pronounced, suggesting $P^2M^2$ coupling is active, but weaker. For fields applied perpendicular to the lamella (parallel to a $[\bar{1}10]_{pc}$ direction), such features are weaker still and, to a first approximation (on the same scale as used in the other two orientations discussed (Figure 4c), $d(C^{-1})/dH$ is almost invariant. However, the absolute magnetocapacitance effect is the strongest of all orientations examined both at 150 K (Figure 2d) and at room temperature (Figure 4d); in fact, the capacitance changes observed are commensurate with the signature of ferroelectric switching seen in our $C(V)$ measurements (Figure 2a), so coupling terms are clearly active. Importantly, this is also the field orientation responsible for the room temperature domain switching illustrated in Figure 1. Such observations point to the decreasing importance of $P^2M^2$ and the increasing importance of asymmetric terms in the magnetoelectric response.

Care should be taken not to view the plots presented in Figure 4 in an overly simplistic manner. The data in Figure 2 show that the value of the measured capacitance changes as magnetic fields are applied for all field orientations. Thus, $d(C^{-1})/dH$ is generally nonzero and hence, even when the magnetic field is applied along $[\bar{1}10]_{pc}$, perpendicular to the lamellar plane, simple $PM$ terms cannot be the sole components. A more complex behavior seems likely, that goes beyond the discussion above, in which explicit strain coupling terms

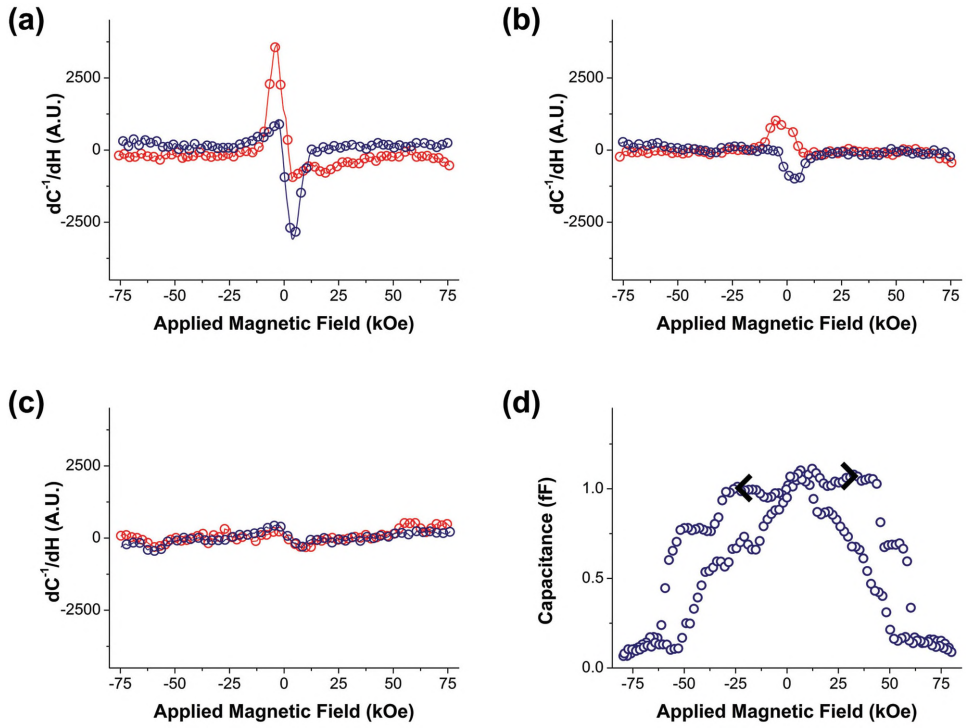


**Figure 4.** Probing the existence and relative magnitude of $P^2M^2$ coupling in PZTFT. Plots of $dC^{-1}/dH$ as a function of magnetic field applied along the $[001]_{pc}$, $[110]_{pc}$ and $[\bar{1}10]_{pc}$ directions (a), b), and c), respectively) in the single crystal lamella coplanar capacitor, at 150 K. Red data points are for increasing field and blue data points for decreasing field. For magnetic fields applied along $[001]_{pc}$ (parallel to the electrode–dielectric interface and in the plane of the lamella), the plot is similar to that of $-M(dM/dH)$ in Figure 3c. This is consistent with measurable $P^2M^2$ coupling. The magnitude of the $P^2M^2$ coupled response is reduced, but still evident, when magnetic fields are along $[110]_{pc}$ (in the plane of the lamella and perpendicular to the electrode–dielectric interface) in (b) and almost imperceptible when the field is along $[\bar{1}10]_{pc}$ (perpendicular to the plane of the lamella) in (c). The minor influence of symmetric $P^2M^2$ behavior for fields along $[\bar{1}10]_{pc}$ is consistent with the observed magnetic field-induced ferroelectric switching, which requires asymmetric coupling terms (such as *PM*). Capacitance still shows a significant dependence on magnetic field in this orientation (not explained by *PM* coupling), even at room temperature d), and so the reality is probably that more complex coupling behavior involving explicit strain terms occurs.

are also active. This would be consistent with the research results reported by Schiemer et al.[26] To be evaluated fully in future work, magnetoelastic changes should be monitored in conjunction with the kinds of magnetoelectric measurements presented and considered here.

Nevertheless, the orientations of the applied magnetic and electric fields, in relation to the possible orientations of polarization in the lamella, should be explicitly considered and are illustrated in **Figure 5**; rhombohedral symmetry, as one of the options postulated by Dilsom et al.,[27] and the development of $[111]_{pc}$ dipole vectors at 150 K are assumed. Applying the magnetic field along $[001]_{pc}$ is distinct by symmetry from the $[110]_{pc}$ and $[\bar{1}10]_{pc}$ directions and so the uniqueness of the strength of the $P^2M^2$ coupling behavior inferred, in comparison to the other two directions, is not surprising. However, one might expect symmetry equivalence in behavior for magnetic fields applied along the $[110]_{pc}$ and $[\bar{1}10]_{pc}$ directions. Such equivalence may indeed be present, but the relative orientation of the electric field used to monitor capacitance is different in the two cases, being parallel to the applied magnetic field in one case and perpendicular to it in the other. The shape of the lamella may also be partly responsible for differences in coupling behavior observed, as depolarizing fields associated with components of polarization perpendicular to the lamellar surface may bias domain populations to favor those with entirely in-plane polar components.

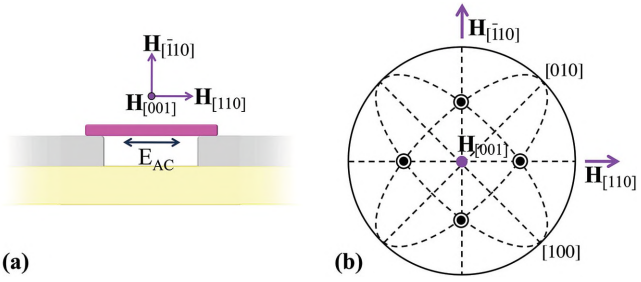


**Figure 5.** Magnetic and electric field directions in relation to suspected polar vector orientations. The directions of the applied magnetic fields in relation to a cross-section of the PZTFT lamella capacitor structure are shown schematically in (a). In (b) is a stereogram of the polar directions (poles plotted using black filled circles and black rings) associated with the rhombohedral ferroelectric domains suspected at 150 K. The orientation of the stereogram in (b) is the same as that of the capacitor cross-section schematic in (a). $H_{[001]}$ is distinct by symmetry from the other two magnetic field directions. However, even the measured magnetocapacitance responses for $H_{[110]}$ and $H_{[\bar{1}10]}$ should be expected to differ, as in one case the sensing electric field is parallel to the applied magnetic field, whereas in the other case, it is perpendicular.

In summary, the ways in which applied magnetic fields change ferroelectric domain states and the dielectric response of single crystal PZTFT lamellae have been investigated. Magnetic fields have been found to induce significant switching of ferroelectric domains, as had been seen previously; in addition, strong magnetocapacitance effects were noted which were different for different orientations of magnetic field. By considering highly generalized Landau free energy expressions, the magnetocapacitance response revealed biquadratic coupling in the plane of the lamellar PZTFT sample; weaker biquadratic coupling was apparent when the magnetic field was perpendicular to the lamella where it was clear that asymmetric coupling terms were more dominant. The study reaffirms that PZTFT genuinely acts as a single-phase room temperature magnetoelectric multiferroic and highlights complexities in the orientational dependence of coupling effects.

## Acknowledgements

J.M.G., J.F.S., and A.S. acknowledge financial support from the Engineering and Physical Sciences Research Council (EPSRC) under research contracts: EP/J017191/1, EP/J017825/1, and EP/H00307X/1. D.M.E., J.M.G., and A.S. acknowledge support from the Northern Ireland Department for Employment and Learning (DEL). D.M.E. and J.M.G. thank R. G. P. McQuaid for helpful discussions.

[1] H. Schmid, *Ferroelectrics* **2012**, *427*, 1.
[2] E. Ascher, H. Rieder, H. Schmid, H. Stossel, *J. Appl. Phys.* **1966**, *37*, 1404.
[3] M. Bibes, *Nat. Mater.* **2012**, *11*, 354.
[4] J. F. Scott, *J. Mater. Chem.* **2012**, *22*, 4567.
[5] S. Roy, S. B. Majumder, *J. Alloys Compd.* **2012**, *538*, 153.
[6] C. A. F. Vaz, *J. Phys.: Condens. Matter* **2012**, *24*, 333201.
[7] V. Skumryev, V. Laukhin, I. Fina, X. Martí, F. Sánchez, M. Gospodinov, J. Fontcuberta, *Phys. Rev. Lett.* **2011**, *106*, 057206.
[8] H. Zheng, J. Wang, S. E. Lofland, Z. Ma, L. Mohaddes-Ardabili, T. Zhao, L. Salamanca-Riba, S. R. Shinde, S. B. Ogale, F. Bai, D. Viehland, Y. Jia, D. G. Schlom, M. Wuttig, A. Roytburd, R. Ramesh, *Science* **2004**, *303*, 661.
[9] F. Zavaliche, H. Zheng, L. Mohaddes-Ardabili, S. Y. Yang, Q. Zhan, P. Shafer, E. Reilly, R. Chopdekar, Y. Jia, P. Wright, D. G. Schlom, Y. Suzuki, R. Ramesh, *Nano Lett.* **2005**, *5*, 1793.
[10] S. Geprägs, A. Brandlmaier, M. Opel, R. Gross, S. T. B. Goennenwein, *Appl. Phys. Lett.* **2010**, *96*, 142509.
[11] I. Levin, J. Li, J. Slutsker, A. L. Roytburd, *Adv. Mater.* **2006**, *18*, 2044.
[12] J. T. Heron, M. Trassin, K. Ashraf, M. Gajek, Q. He, S. Y. Yang, D. E. Nikonov, Y.-H. Chu, S. Salahuddin, R. Ramesh, *Phys. Rev. Lett.* **2011**, *107*, 217202.
[13] T. H. E. Lahtinen, K. J. A. Franke, S. van Dijken, *Sci. Rep.* **2012**, *2*, 258.
[14] T. Kimura, T. Goto, H. Shintani, K. Ishizaka, T. Arima, Y. Tokura, *Nature* **2003**, *406*, 55.
[15] N. Hur, S. Park, P. A. Sharma, J. S. Ahn, S. Guha, S.-W. Cheong, *Nature* **2004**, *429*, 392.
[16] M. Fiebig, Th. Lottermoser, D. Fröhlich, A. V. Goltsev, R. V. Pisarev, *Nature* **2002**, *419*, 818.
[17] Z. J. Huang, Y. Cao, Y. Y. Sun, Y. Y. Xue, C. W. Chu, *Phys. Rev. B* **1997**, *56*, 2623.
[18] V. Scagnoli, U. Staub, Y. Bodenthin, R. A. de Souza, M. García-Fernández, M. Garganourakis, A. T. Boothroyd, D. Prabhakaran, S. W. Lovesey, *Science* **2011**, *332*, 696.
[19] T. Kimura, Y. Sekio, H. Nakamura, T. Siegrist, A. P. Ramirez, *Nat. Mater.* **2008**, *7*, 291.
[20] J. H. Lee, L. Fang, E. Vlahos, X. Ke, Y. W. Jung, L. F. Kourkoutis, J.-W. Kim, P. J. Ryan, T. Heeg, M. Roeckerath, V. Goian, M. Bernhagen, R. Uecker, P. C. Hammel, K. M. Rabe, S. Kamba, J. Schubert, J. W. Freeland, D. A. Muller, C. J. Fennie, P. Schiffer, V. Gopalan, E. Johnston-Halperin, D. G. Schlom, *Nature* **2010**, *466*, 954.
[21] J. T. Heron, J. L. Bosse, Q. He, Y. Gao, M. Trassin, L. Ye, J. D. Clarkson, C. Wang, J. Liu, S. Salahuddin, D. C. Ralph, D. G. Schlom, J. Íñiguez, B. D. Huey, R. Ramesh, *Nature* **2014**, *516*, 370.
[22] L. Keeney, T. Maity, M. Schmidt, A. Amann, N. Deepak, N. Petkov, S. Roy, M. E. Pemble, R. W. Whatmore, *J. Am. Ceram. Soc.* **2013**, *96*, 2339.
[23] S. Mukherjee, A. Roy, S. Auluck, R. Prasad, R. Gupta, A. Garg, *Phys. Rev. Lett.* **2013**, *111*, 087601.
[24] D. M. Evans, A. Schilling, A. Kumar, D. Sanchez, N. Ortega, M. Arredondo-Arechavala, R. Katiyar, J. M. Gregg, J. F. Scott, *Nat. Commun.* **2013**, *4*, 1534.
[25] D. M. Evans, A. Schilling, Ashok Kumar, D. Sanchez, N. Ortega, R. S. Katiyar, J. F. Scott, J. M. Gregg, *Philos. Trans. R. Soc., A* **2014**, *372*, 2009.
[26] J. Schiemer, M. A. Carpenter, D. M. Evans, J. M. Gregg, A. Schilling, M. Arredondo, M. Alexe, D. Sanchez, N. Ortega, R. S. Katiyar, M. Echizen, E. Colliver, S. Dutton, J. F. Scott, *Adv. Funct. Mater.* **2014**, *24*, 2993.
[27] D. A. Sanchez, N. Ortega, A. Kumar, R. Roque-Malherbe, R. Polanco, J. F. Scott, R. S. Katiyar, *AIP Adv.* **2011**, *1*, 042169.
[28] D. A. Sanchez, N. Ortega, A. Kumar, G. Sreenivasulu, R. S. Katiyar, J. F. Scott, D. M. Evans, M. Arredondo-Arechavala, A. Schilling, J. M. Gregg, *J. Appl. Phys.* **2013**, *133*, 074105.
[29] R. O. Kuzian, V. V. Laguta, J. Richter, *Phys. Rev. B* **2014**, *90*, 134415.
[30] R. O. Kuzian, I. V. Kondakova, A. M. Daré, V. V. Laguta, *Phys. Rev. B* **2014**, *89*, 024402.
[31] M. D. Glinchuk, E. A. Eliseev, A. N. Morozovska, *J. Appl. Phys.* **2014**, *116*, 054101.
[32] R. G. P. McQuaid, L. J. McGilly, P. Sharma, A. Gruverman, J. M. Gregg, *Nat. Comms.* **2011**, *2*, 404.
[33] P. Sharma, R. G. P. McQuaid, L. J. McGilly, J. M. Gregg, A. Gruverman, *Adv. Mater.* **2013**, *25*, 1323.
[34] L. W. Chang, M. McMillen, F. D. Morrison, J. F. Scott, J. M. Gregg, *Appl. Phys. Lett.* **2008**, *93*, 132904.
[35] G. Catalan, *Appl. Phys. Lett.* **2006**, *88*, 102902.
[36] D. L. Fox, D. R. Tilley, J. F. Scott, H. J. Guggenheim, *Phys. Rev. B* **1980**, *21*, 2926.
[37] W. Peng, N. Lemée, J. Holc, M. Kosec, R. Blinc, M. G. Karkut, *J. Magn. Magn. Mater.* **2009**, *321*, 1754.